

H_2^+ and HeH: approximating potential curves, rovibrational states

Horacio Olivares-Pilón*

*Departamento de Física, Universidad Autónoma Metropolitana-Iztapalapa,
Apartado Postal 55-534, 09340 México, D.F., Mexico*

Alexander V. Turbiner†

*Instituto de Ciencias Nucleares, Universidad Nacional Autónoma de México,
Apartado Postal 70-543, 04510 México, D.F., Mexico*

Abstract

It is shown that in the Bohr-Oppenheimer approximation for four lowest electronic states $1s\sigma_g$ and $2p\sigma_u$, $2p\pi_u$ and $3d\pi_g$ of H_2^+ and the ground state $X^2\Sigma^+$ of HeH, the potential curves can be well-approximated analytically in full range of internuclear distances R with not less than 4-5-6 figures. Approximation is based on straightforward interpolation of the Taylor-type expansion at small R and a combination of the multipole expansion with one-instanton type expansion at large distances R . The position of minimum when exists is predicted within 1% (or better).

For the molecular ion H_2^+ in the Lagrange mesh method, the spectra of vibrational, rotational and rovibrational states (ν, L) associated with $1s\sigma_g$ and $2p\sigma_u$, $2p\pi_u$ and $3d\pi_g$ analytically derived potential curves is calculated. In general, it coincides with spectra found via numerical solution of the Schrödinger equation when available. It is shown that $1s\sigma_g$ curve contains 19 vibrational states $(\nu, 0)$, while $2p\sigma_u$ curve contains a single one $(0, 0)$ and $2p\pi_u$ state contains 12 vibrational states $(\nu, 0)$. In general, $1s\sigma_g$ electronic curve contains 420 rovibrational states, which increases up to 423 when beyond BO approximation. For the state $2p\sigma_u$ the total number of rovibrational states (all with $\nu = 0$) is equal to 3 within or beyond Bohr-Oppenheimer approximation. As for the state $2p\pi_u$ within the Bohr-Oppenheimer approximation the total number of the rovibrational bound states is equal to 284. The state $3d\pi_g$ is repulsive.

It is confirmed in Lagrange mesh formalism the statement that the ground state curve of the heteronuclear molecule (HeH) does not support rovibrational states.

*Electronic address: horop@xanum.uam.mx

†Electronic address: turbiner@nucleares.unam.mx

INTRODUCTION

A chance to "integrate out" effectively the electronic degrees of freedom is a remarkable feature of the Bohr-Oppenheimer approximation. The original problem say for simplicity of diatomic molecule is reduced to two-body problem in an effective potential called *the (electronic) potential curve* $V(R)$,

$$\mathcal{H}(R) = \frac{P^2}{2} + V(R) + \frac{L(L+1)}{R^2}, \quad (1)$$

which describes nuclear motion, here L is angular momentum, the reduced mass for simplicity is placed equal to one and $P = -i\nabla_R$, $\hbar = 1$. The (electronic) potential curve $V(R)$ depends on the original state of the diatomic molecule and usually is known numerically. It was a challenge for a long time to find out how to interpolate analytically the potential curves with sufficiently high accuracy in full range of internuclear distances.

The H_2^+ molecular ion plays a fundamental role in different physics sciences: atomic-molecular physics, in laser and plasma physics being also a traditional example of two-center Coulomb system of two heavy Coulomb charges Z and electron, (Z, Z, e) in Quantum Mechanics (see e.g. [1]). It represents the simplest diatomic molecule. Due to the fact that the proton is much heavier than electron the problem is usually explored in the static approximation - the Bohr-Oppenheimer approximation of the zero order - where the protons are assumed to be infinitely heavy. In general, the projection of the angular momentum to the molecular axis (the line connecting the proton positions) L_ϕ is the integral, $[L_\phi, \mathcal{H}] = 0$, where \mathcal{H} is the Hamiltonian. Thus, the angular variable ϕ can be separated out. Hence, the problem is reduced to two-dimensional, which admits itself the separation of variables in elliptic coordinates. It reflects the outstanding property of the general two-center Coulomb problem (Z_1, Z_2, e) of the complete separation of variables in prolate ellipsoidal coordinates. Thus, the problem is (completely)-integrable. Contemporary theory of low-lying states of H_2^+ in the Bohr-Oppenheimer approximation (electronic structure and radiative transitions) is presented at [2]. It is based on highly accurate locally approximation of the lowest eigenfunctions proposed in [3]. However, potential curves of the electronic states remained known numerically.

In turn, (HeH) is the simplest neutral heteroatomic molecule. It was intensely studied numerically, see e.g. [4] and references therein, where a shallow van der Waals minimum

was found. In general, it is as unstable and the ground state potential curve is repulsive.

Present paper is aimed to construct simple analytic approximations of potential curves of the low-lying electronic states of H_2^+ and (HeH) in full range of internuclear distances, which reproduce not less than 4-5-6 figures in numerically-found potential curves. The same time we require that the spectra in potential curves is reproduced with not less than 6 figures.

Based on that we develop the theory of vibrational and rotational states for a few low-lying electronic states for H_2^+ and for the ground state potential curve of (HeH) .

Atomic units are used throughout, in particular, for distances, although the energy is given in Rydbergs.

I. GENERALITIES: THE MOLECULAR ION H_2^+

The Schrödinger equation, which describes the electron in the field of two fixed centers of the charges Z_1, Z_2 at the distance R , is of the form

$$\left(-\Delta - \frac{2Z_1}{r_1} - \frac{2Z_2}{r_2}\right)\Psi = E'\Psi, \quad \Psi \in L^2(\mathbf{R}^3), \quad (2)$$

where $E' = (E - \frac{2Z_1Z_2}{R})$ and the total energy $E(R)$ are both in Rydbergs, $r_{1,2}$ are the distances from electron to first (second) center, respectively, see Fig. 1, both are in a.u. From physical point of view, we study the motion of electron in the field of two Coulomb wells situated on the distance R . If $Z_1 = Z_2$ the wells become identical - any eigenstate is characterized by a definite parity with respect to permutation of wells (centers). Furthermore, at $R \rightarrow \infty$, when the barrier gets large and tunneling becomes exponentially-small, the phenomenon of pairing should occur: the spectra of positive parity states is almost degenerate with the spectra of negative parity states, asymptotically both are equal to the energy spectra of hydrogen atom E_H . For each pair the energy gap should be exponentially-small, $\sim e^{-aR}$ where a is a parameter. Dissociation energy is given by

$$\tilde{E} = E(R) - E_H. \quad (3)$$

We focus on the case of unit charges $Z_1 = Z_2 = 1$ - the only case where bound states occur - it corresponds to H_2^+ molecular ion.

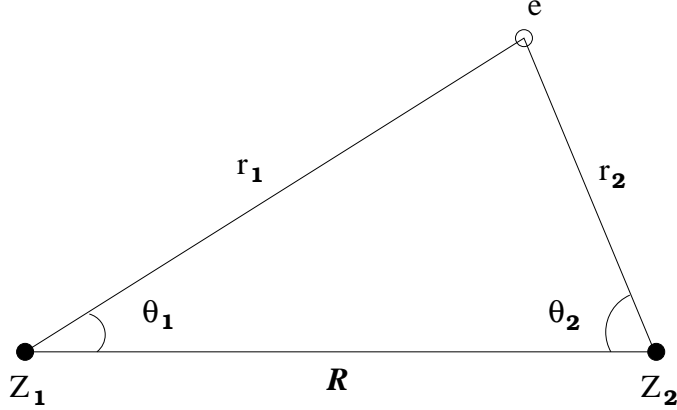


FIG. 1: Geometrical settings for (Z_1, Z_2, e) .

II. H_2^+ : THE LOWEST STATES POTENTIAL CURVES

A. Energy gap between $1s\sigma_g$ and $2p\sigma_u$ states

The Born-Oppenheimer approximation leads to the concept of electronic potential curve, which has the meaning of the total energy of the system H_2^+ at fixed internuclear distance R . Thus, the problem to find a potential curve is reduced to finding spectra of electronic Schrödinger equation (2), where R plays a role of parameter. Since the potential in (2) is a double-well potential with degenerate minima, it is natural to study the energy gap, which is the distance between two lowest eigenstates,

$$\Delta E = E_{2p\sigma_u} - E_{1s\sigma_g} . \quad (4)$$

The goal of the Sections II.A-B is to refine the results obtained in [2].

For small R it was found long ago the expansion with finite radius of convergence [5–7] [21]

$$\Delta E = 3 - \frac{82}{15}R^2 + \frac{32}{3}R^3 + O(R^4) , \quad (5)$$

while at large R the corresponding expansion [8–10],

$$\Delta E = \frac{8}{e}R e^{-R} \left(1 + \frac{1}{2R} - \frac{25}{8R^2} + \dots \right) + O(e^{-2R}). \quad (6)$$

It looks like the multi-instanton expansion where R plays a role of the classical action. Seemingly, the series in pre-factor is asymptotic - it has zero radius of convergence in $1/R$.

Now we take data for potential curves of the $1s\sigma_g$ and $2p\sigma_u$ states, see Tables 1,2 [2], calculate the difference ΔE and interpolate between small and large distances using the

Padé type approximation $e^{-R-1} \text{Pade}[N + 1/N](R)$, where $\text{Pade}[N + 1/N](R)$ is meromorphic function, $p_{N+1}(R)/q_N(R)$. In general, ΔE is smooth, slow-changing curve with R , exponentially-vanishing at $R \rightarrow \infty$, see below Fig. 2.

Taking several different values N we found that $N = 7$ is the smallest which provides the quality of fit we would like to have, see below,

$$\Delta E = e^{-R-1} \text{Pade}[8/7](R) ,$$

or explicitly,

$$\Delta E = e^{-R-1} \frac{3e + a_1 R + a_2 R^2 + a_3 R^3 + a_4 R^4 + a_5 R^5 + a_6 R^6 + a_7 R^7 + 8R^8}{1 + \alpha_1 R + \alpha_2 R^2 + b_3 R^3 + b_4 R^4 + b_5 R^5 + \alpha_3 R^6 + R^7} , \quad (7)$$

where three constraints

$$\begin{aligned} \alpha_1 &= (a_1 - 3e)/(3e) , \\ \alpha_2 &= (-a_1 + a_2 + \frac{209e}{30})/(3e) , \\ \alpha_3 &= (a_7 - 4)/8 , \end{aligned} \quad (8)$$

are imposed, which guarantee that the appropriate expansions of (7) reproduce correctly the R^0 , R^1 and R^2 terms in (5) and the two terms in (6). Eventually, (7) has ten free parameters which are fixed by making fit of numerical data with (7) with minimal χ^2 . As the result those ten free parameters take values:

$$\begin{aligned} a_1 &= 446.5741 , & a_6 &= 214.0609 , \\ a_2 &= 905.1538 , & a_7 &= -52.89581 , \\ a_3 &= 223.2718 , & b_3 &= 38.57209 , \\ a_4 &= 307.0596 , & b_4 &= -38.28025 , \\ a_5 &= -235.4166 , & b_5 &= 31.65441 , \end{aligned} \quad (9)$$

where the seven shown figures are significant. Note that the parameters (9) are much smaller than ones find in [2]. This fit gives, in general, 6-7 figures at the whole range $R \in [0, 40]$ a.u., see Table I, and furthermore, up to 9 d.d. for large $R \in [20, 40]$ a.u. (see for illustration Table I and Fig. 2, blue curve). Saying differently, the largest absolute difference between exact and fitted energy gaps occurs at 5th decimal digit in domain $R \in [0.5, 9.0]$ a.u. It gets even more accurate outside of this domain.

TABLE I: E_0 (13) and ΔE (4) between the ground $1s\sigma_g$ and first excited state $1s\sigma_g$ and $2p\sigma_u$ of the molecular ion H_2^+ in Ry as a function of the internuclear distance R compared to the results of the fits (16) and (7).

R	$E_0 = \frac{1}{2}(E_{2p\sigma_u} + E_{1s\sigma_g}) + 1$		$\Delta E = E_{2p\sigma_u} - E_{1s\sigma_g}$	
	data	Fit (16)	data	Fit (7)
0.1	18.5210904842	18.521096	2.9551492517	2.955137
0.5	2.7481265348	2.748074	2.4362050695	2.436192
1.0	0.9834000615	0.983519	1.7739453766	1.773930
2.0	0.2298313933	0.229534	0.8701996446	0.870186
3.0	0.0543521359	0.054627	0.4189557280	0.418955
4.0	0.0083644769	0.008011	0.2010684887	0.201072
5.0	-0.0017119084	-0.001535	0.0942573639	0.094260
6.0	-0.0026129408	-0.002134	0.0426503122	0.042641
7.0	-0.0018657168	-0.001514	0.0186445834	0.018645
8.0	-0.0011764042	-0.000989	0.0079287460	0.007935
9.0	-0.0007392824	-0.000649	0.0033032469	0.003309
10.0	-0.0004797975	-0.000437	0.0013553207	0.001359
30.0	-5.581483×10^{-6}	-5.569×10^{-6}	$< 10^{-10}$	$< 10^{-10}$

B. The ground state $1s\sigma_g$ and the first excited state $2p\sigma_u$

For the lowest state $1s\sigma_g$, the behavior of the potential curve $E_{1s\sigma_g}$ at the two asymptotic limits of small and large distances is well known. For $R \rightarrow 0$ the dissociation energy is given by [5–7]

$$\tilde{E}_{1s\sigma_g}^{(0)} = \frac{2}{R} - 3 + \frac{16}{3}R^2 - \frac{32}{3}R^3 + O(R^4 \log R), \quad (10)$$

it can be found in perturbation theory in powers of R . Note the linear in R term is absent. In turn, for the dissociation energy at $R \rightarrow \infty$ the expansion reads [8–10]

$$\begin{aligned} \tilde{E}_{1s\sigma_g}^{(\infty)} = & -\frac{9}{2R^4} - \frac{15}{R^6} - \frac{213}{2R^7} + \dots \\ & -4R e^{-R-1} \left[1 + \frac{1}{2R} - \frac{25}{8R^2} - \frac{131}{48R^3} - \frac{3923}{384R^4} + \dots \right] + O(e^{-2R}), \end{aligned} \quad (11)$$

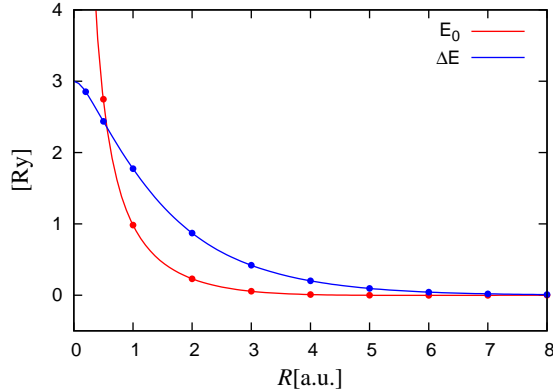


FIG. 2: E_0 and ΔE for $1s\sigma_g$ and $2p\sigma_u$ states as defined by (13) and (4), respectively. Calculated energies are marked by dots, the solid curves are the fits (16) (red) and (7) (blue), c.f. Fig. 4 in [2].

where the first sum represents the multipole expansion, the second one is a type of one-instanton contribution etc. Note that in the multipole expansion the term R^{-5} (next-after-leading) is absent.

As for the lowest state of the negative parity $2p\sigma_u$ large and small R -distance expansions are known as well,

$$\tilde{E}_{2p\sigma_u}^{(0)} = \frac{2}{R} - \frac{2}{15}R^2 + \dots, \quad (12)$$

at $R \rightarrow 0$, where the next-after-leading terms, $O(1)$ and $O(R)$, are absent, see [15]. The behavior for $R \rightarrow \infty$ is the same as one given by Eq. (11) with sign changed from minus to plus in front of the exponentially-small term $\sim e^{-R}$.

Let us consider the sum of potential curves for $1s\sigma_g$ and $2p\sigma_u$ states,

$$E_0 \equiv \frac{\tilde{E}_{1s\sigma_g} + \tilde{E}_{2p\sigma_u}}{2}. \quad (13)$$

Its corresponding expansions are

$$E_0 = \frac{2}{R} - \frac{3}{2} + \frac{13}{5}R^2 + \dots, \quad (14)$$

at $R \rightarrow 0$, see [15], where the linear in R term is absent, and

$$E_0 = -\frac{9}{2R^4} - \frac{15}{R^6} - \frac{213}{2R^7} + \dots + O(e^{-2R}), \quad (15)$$

at $R \rightarrow \infty$, where again the term R^{-5} is absent. The first expansion (14) has a finite radius of convergence, see e.g. [6], while the second one (15) (the halfsum of two multipole expansions) has zero radius of convergence.

Now we assume that two-instanton contribution, $\sim e^{-2R}$ at large R (and possible higher exponentially-small contributions), can be neglected and construct the analytic approximation for E_0 which mimics the two asymptotic limits (14), (15). The most convenient way to do it is to use Padé type approximation (ratio of two polynomials) $E_0(R) = \frac{1}{R}$ Pade[$N/N+3$](R) with a certain N . Concrete fit was made for $N = 5$, where the Padé approximation is of the form $E_0(R) = \frac{1}{R}$ Pade[5/8](R),

$$E_0 = \frac{2 + a_1R + a_2R^2 + a_3R^3 + a_4R^4 - 9R^5}{R(1 + \alpha_1R + \alpha_2R^2 + b_3R^3 + b_4R^4 + b_5R^5 - \alpha_3R^6 - \alpha_4R^7 + 2R^8)} , \quad (16)$$

with four constraints imposed,

$$\begin{aligned} \alpha_1 &= (a_1 + 3/2)/2 , \\ \alpha_2 &= (6a_1 + 8a_2 + 9)/16 , \\ \alpha_3 &= 2(a_3 + 30)/9 , \\ \alpha_5 &= 2a_4/9 , \end{aligned} \quad (17)$$

see below, thus, (16) depends on seven free parameters. Above constraints guarantee that the three coefficients in front of R^{-1} , R^0 and R^1 of expansion at $R \rightarrow 0$, see (14) and the three coefficients in front of R^{-4} , R^{-5} and R^{-6} at $R \rightarrow \infty$, in the $1/R$ -expansion (15) are all exact. After making the fit with (16), we arrive to concrete values of these seven free parameters:

$$\begin{aligned} a_1 &= 267.095 , & b_3 &= 124.971 , \\ a_2 &= 375.335 , & b_4 &= -57.4398 , \\ a_3 &= -180.965 , & b_5 &= 10.5173 , \\ a_4 &= 60.700 , \end{aligned} \quad (18)$$

c.f. (47) in [2]. It provides not less than 5-6 figures in E_0 for whole studied domain $R \in [1, 40]$ a.u., see Table I and Fig. 2. Saying differently, the largest absolute difference between exact and fitted energies occurs at 5th decimal digit in domain $R \in [0.5, 9.0]$ a.u. It gets smaller outside of this domain.

The potential curve for the ground state $1s\sigma_g$ can be constructed from (16) and (7) by taking

$$E_{1s\sigma_g} = E_0 - \frac{1}{2}\Delta E . \quad (19)$$

This expression reproduces 4-5-6 figures in energy for the whole domain $R \in [0, 40]$ a.u., when comparing with the exact values, see Table 1 [2], for illustration see Fig. 3. It differs

in 5-6 figure. It is quite remarkable that the minimum of the potential curve is predicted at $E_{min}^{(fit)} = -1.20556$ Ry (c.f. $E_{min}^{exact} = -1.20527$ Ry) while its location is $R_{eq}^{(fit)} = 1.99684$ a.u. (c.f. $R_{eq}^{exact} = 1.99719$ a.u.).

The asymptotic expansions of Eq. (19) are given by

$$\tilde{E}_0 = \frac{2}{R} - 3 + 4.413 R^2 + \dots, \quad (20)$$

$$\tilde{E}_\infty = -\frac{9}{2R^4} - \frac{15}{R^6} + \frac{110.166}{R^7} + \dots - 4Re^{-R-1} \left[1 + \frac{1}{2R} - \frac{1.3408}{R^2} \dots \right], \quad (21)$$

which are in complete agreement with the first three terms at $R \rightarrow 0$, and with the first three terms in the $1/R$ expansion and two terms in $1/R$ expansion of the pre-factor to e^{-R} for $R \rightarrow \infty$ (cf. (10) and (11)).

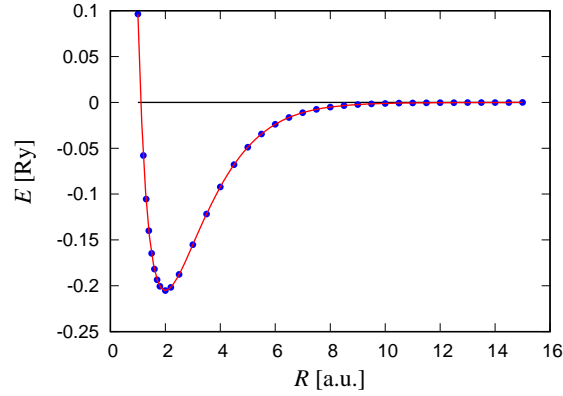


FIG. 3: Potential curve for the ground state $1s\sigma_g$: points are the calculated values and the solid curve is the fit (19), c.f. Fig.5 in [2].

Similarly, the potential curve for the excited state $2p\sigma_u$ is restored from (16) and (7) by taking

$$E_{2p\sigma_u} = E_0 + \frac{1}{2} \Delta E. \quad (22)$$

This expression also reproduces 4-5-6 figures when comparing with the exact energy, see Table 2 in [2] and for illustration Fig. 4. The asymptotic expansions of Eq. (22) are given by

$$\tilde{E}_0 = \frac{2}{R} - 1.0536 R^2 + \dots, \quad (23)$$

$$\tilde{E}_\infty = -\frac{9}{2R^4} - \frac{15}{R^6} + \frac{110.166}{R^7} + \dots + 4Re^{-R-1} \left[1 + \frac{1}{2R} - \frac{1.3408}{R^2} \dots \right], \quad (24)$$

which are in complete agreement with the first three terms at $R \rightarrow 0$ (cf. (10)), and three terms in $1/R$ expansion and two terms in $1/R$ expansion of the pre-factor to e^{-R} for $R \rightarrow \infty$ (cf. (11)).

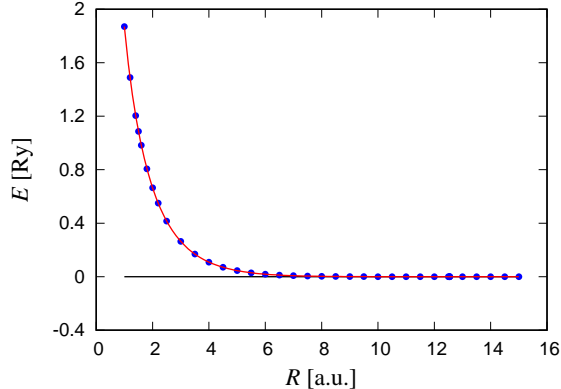


FIG. 4: Potential curve for the lowest state of negative parity $2p\sigma_u$: the calculated values are marked by dots and the solid curve represents the fit (22), c.f. Fig.6 in [2].

C. Rovibrational states associated with the ground state curve $1s\sigma_g$

Inside of the Born-Oppenheimer approximation the knowledge of potential electronic curve for $1s\sigma_g$ allows us to find the vibrational and rotational as well as rovibrational states by solving the equation

$$\left[-\frac{1}{\mu} \frac{d^2}{dR^2} + \frac{L(L+1)}{\mu R^2} + V(R) \right] \phi(R) = E_{\nu L} \phi(R), \quad (25)$$

where $\mu = M_p/2$ is the reduced mass of the two protons, $V(R)$ is the total electronic energy for $1s\sigma_g$, ν and L are the vibrational and rotational quantum numbers, respectively. In particular, the analytic approximation for the potential curve $V(R) = E_{1s\sigma_g}(R)$ (19) made out the expressions (16) and (7) allows us to calculate the rovibrational energies $E_{\nu L}$ associated with the bound state $1s\sigma_g$ for different values of ν and L . It is done by solving the one-dimensional differential equation (25) using the Lagrange-mesh method, see e.g. [11]. Then the spectra can be compared with a numerical solution of the Schrödinger equation (25) with numerically-defined potential $V(R)$. Simple estimate shows that the energy spectra differ obtained in these two methods should differ in 6th figure (or beyond).

Table II presents the obtained vibrational states for $L = 0$ until $L = 35$ in increasing steps of 5; the proton reduced mass $\mu = 918.048$ is taken. For $L = 0$, second column displays

the results as given by Beckel *et al.* [12]. In general, the agreement when comparing with our results is within 10^{-3} . In all cases the first column, second lines show the rovibrational energies calculated by Moss [13], but where the finite mass effects are taken into account, thus, being beyond BO approximation. It must be noted that this finite mass effects due to finiteness of the proton and electron masses usually change the fifth figure in the energy. It indicates the real accuracy of the Born-Oppenheimer approximation, which is four figures. Hence, it seems physically *irrelevant* to find potential curves with more than five figures (as it was done in the past, in particular, in [12]), when we are in static approximation. Note that beyond static approximation the potential curves do not exist(!).

In general, our approximation in the most cases agrees with old results by Beckel *et al.* [12] for $L = 0$ within four-five figures - it provides relevant description of spectra of vibrational states H_2^+ within applicability of non-relativistic quantum mechanics in the Born-Oppenheimer approximation. Note our spectra also agrees with results by Moss [13] within five figures!

Note that the existence of 20th vibrational state predicted by Moss with binding energy $\sim 6 \times 10^{-6}$ a.u. goes beyond the applicability of Born-Oppenheimer approximation. Thus, the result obtained in [12] can not be trusted. We should conclude that within the Born-Oppenheimer approximation the potential curve for $1s\sigma_g$ state keeps 19 vibrational states. Taking into account the finite mass corrections the number of vibrational states increases to 20.

For $L > 0$ the agreement between our results in BO approximation and those by Moss [13] reduces to four and even (sometimes) to three figures, see Table II. Maximum angular momentum L , which still keeps vibrational bound state, is equal to $L_{max} = 35$. It keeps a single vibrational state with $\nu = 0$ with dissociation energy 0.00541 Ry. For $L > 35$ rovibrational bound states occur neither in BO approximation nor beyond [22].

Figure 5 displays the 420 rovibrational bound states supported by the ground state potential calculated in the Lagrange mesh method. Note that beyond the Born-Oppenheimer approximation in [13] it is reported 423 bound states. The total number of vibrational bound states for each value of the angular momentum L is presented by the histogram on Figure 6.

TABLE II: Rovibrational states $E_{\nu,L}$ of the ground electronic state $1s\sigma_g$ of the molecular ion H_2^+ , all energies are in Ry. For $E_{\nu 0}$ (the first two columns) comparison of our results (first line, first column) is done with Moss [13] (non-adiabatic, rounded) (second line, first column) and with Beckel *et al.* [12], (adiabatic, second line, second column). For $L = 5, \dots, 35$ our results (first lines) are compared with [13] (second lines)

ν	$E_{\nu 0}$ [Ry]	[12]	$E_{\nu,5}$ [Ry]	$E_{\nu,10}$ [Ry]	$E_{\nu,15}$ [Ry]	$E_{\nu,20}$ [Ry]	$E_{\nu,25}$ [Ry]	$E_{\nu,30}$ [Ry]	$E_{\nu,35}$ [Ry]
0	-1.19498		-1.18715	-1.16765	-1.13954	-1.10638	-1.07137	-1.03707	-1.00541
	-1.194278126	-1.194791662	-1.186463458	-1.167016413	-1.139029777	-1.106023726	-1.071105378	-1.036724792	-1.004827669
1	-1.17484		-1.16742	-1.14898	-1.12248	-1.09134	-1.05859	-1.02662	
	-1.174311358	-1.174816204	-1.166909592	-1.148504500	-1.122055804	-1.090936653	-1.058146451	-1.026104261	
2	-1.15593		-1.14892	-1.13152	-1.10659	-1.07738	-1.04676	-1.01707	
	-1.155503809	-1.156001122	-1.148500959	-1.131104266	-1.106150004	-1.076878002	-1.046197512	-1.016526876	
3	-1.13822		-1.13162	-1.11523	-1.09180	-1.06442	-1.03587	-1.00851	
	-1.137816998	-1.138307912	-1.131201173	-1.114784779	-1.091290018	-1.063837402	-1.035266103	-1.008036780	
4	-1.12166		-1.11544	-1.10003	-1.07804	-1.05243	-1.02593	-1.00107	
	-1.121218442	-1.121704068	-1.114979816	-1.099521038	-1.077459594	-1.051811463	-1.025370105	-1.000705972	
5	-1.10619		-1.10034	-1.08586	-1.06526	-1.04140	-1.01701		
	-1.105681500	-1.106162942	-1.099812309	-1.085293962	-1.064648793	-1.040804555	-1.016540673		
6	-1.09175		-1.08626	-1.07269	-1.05345	-1.03136	-1.00919		
	-1.091185303	-1.091663658	-1.085679891	-1.072090485	-1.052854375	-1.030830002	-1.008827534		
7	-1.07831		-1.07316	-1.06049	-1.04262	-1.02234	-1.00258		
	-1.077714775	-1.078191152	-1.072569685	-1.059903774	-1.042080401	-1.021912007	-1.002309928		
8	-1.06584		-1.06105	-1.04927	-1.03280	-1.01442			
	-1.065260759	-1.065736280	-1.060474876	-1.048733603	-1.032339167	-1.014088887			
9	-1.05435		-1.04991	-1.03905	-1.02402	-1.00768			
	-1.053820249	-1.054296054	-1.049395017	-1.038586924	-1.023652626	-1.007419055			
10	-1.04386		-1.03977	-1.02985	-1.01634	-1.00223			
	-1.043396739	-1.043873998	-1.039336482	-1.029478689	-1.016054657	-1.001994126			
11	-1.03438		-1.03067	-1.02173	-1.00984				
	-1.034000731	-1.034480660	-1.030313104	-1.021433071	-1.009594965				
12	-1.02596		-1.02263	-1.01473	-1.00459				
	-1.025650407	-1.026134274	-1.022347044	-1.014485285	-1.004346762				
13	-1.01863		-1.01571	-1.00892	-1.00072				
	-1.018372497	-1.018861640	-1.015469986	-1.008684516	-1.000426364				
14	-1.01244		-1.00996	-1.00436					
	-1.012203363	-1.012699212	-1.009724738	-1.004099214					
15	-1.00744		-1.00544	-1.00117					
	-1.007190171	-1.007694280	-1.005167397	-1.000829395					
16	-1.00370		-1.00221						
	-1.003391547	-1.003905608	-1.001870025						
17	-1.00127		-1.00037						
	-1.000874081	-1.001399856							
18	-1.00017								
	-0.999674864	-1.000213178							
19	—								
	-0.999462461	-1.000006426							

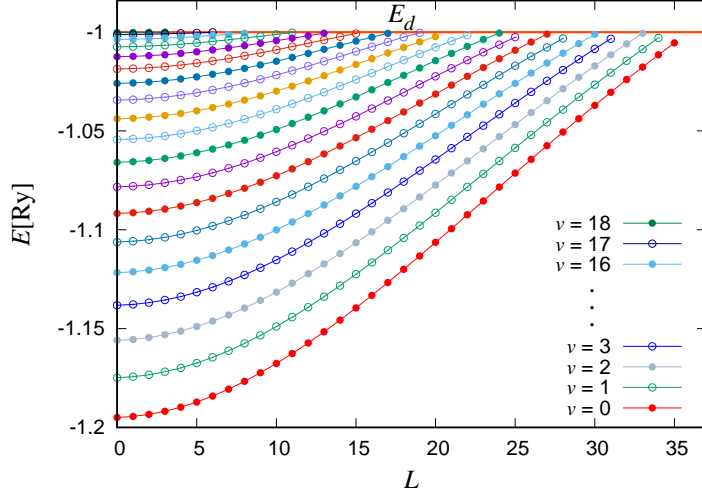


FIG. 5: Rovibrational bound states supported in the ground state $1s\sigma_g$ of the molecular ion H_2^+ in the Born-Oppenheimer approximation. Each point represent the state with angular momentum L and vibrational quantum number ν . The dissociation energy $E_d = -1.0$ Ry.

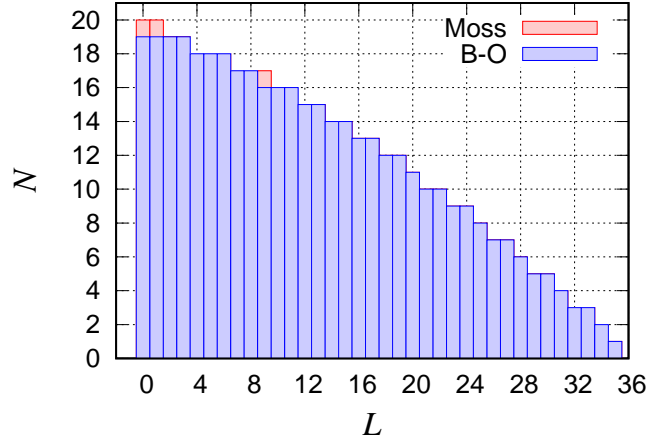


FIG. 6: Number of rovibrational bound states in the ground state $1s\sigma_g$ of the molecular ion H_2^+ as a function of the angular momentum L . The three extra bound states reported in [13] are indicated in red.

1. *The first excited state $2p\sigma_u$*

In the same way as for the ground state $1s\sigma_g$ one can analyze the first excited state $2p\sigma_u$ using for the analytic potential (22) in framework of the equation (25). It is well known from the highly-accurate calculations that the $2p\sigma_u$ potential curve at the large internuclear distance $R = 12.545\,25$ a.u. displays a shallow minimum, $E_t = -1.000\,122$ Ry, see e.g.[3].

TABLE III: Vibrational (ν) and rotational energies in Ry (L) for the first electronic excited state $2p\sigma_u$. Comparison with Peek [14] and those for the full geometry three body system given by Moss [13] presented (rounded)

ν	L	$E_{\nu L}[\text{Ry}]$	[14]	[13]
0	0	-1.00003	-1.000031268	-0.999487004
0	1	-1.00002	-1.000022797	-0.999478536
0	2	-1.00001	-1.000007307	-0.999463045
E_{diss}	-1.0	-1.0		-0.999455679

Taking the first derivative of our approximate potential curve (22) equal to zero it is found a minimum at $R = 12.7034$ a.u. with $E_t = -1.000114$ Ry. Although the position of the minima is determined with relative accuracy $\sim 10^{-2}$, the depth of the well is found with relative accuracy $\sim 10^{-5}$. The vibrational and rotational states supported by this shallow minima can be calculated by solving (25). Table III presents the results obtained for the three rotational states $L = 0, 1, 2$ with vibrational quantum number $\nu = 0$, calculated with $\mu = 918.048$. No states with $\nu > 0$ are seen even though in [14] is presented a state with $\nu = 1$, this is beyond the accuracy of the Bohr-Oppenheimer approximation. Results by Peek [14] and by Moss [13] are presented for comparison. Evidently even taking the most accurate value of the proton to electron mass ratio $\mu = 918.076336945$ does not change our agreement with [14]. The presented spectra of these states agree with results in [14] within six figures and correspond to weak-bound states with extremely-small binding energy of $10^{-5} - 10^{-6}$ a.u. These results for energies are definitely beyond the domain of applicability of the Born-Oppenheimer approximation: finite-mass corrections change the fifth figure, see Table III. Thus, the question about the existence of three rotational bound states associated with $2p\sigma_u$ potential curve remains open in the Born-Oppenheimer approximation. However, taking into account the finite-mass effects [13] leads to the conclusion that three rotational bound states $L = 0, 1, 2$ with vibrational quantum number $\nu = 0$ do exist. It is quite surprising that so much shallow well keeps vibrational bound states.

D. The excited states $2p\pi_u$ and $3d\pi_g$

Let us consider now the excited states $2p\pi_u$ and $3d\pi_g$. Interestingly, at large internuclear distances these states are almost degenerate.

The expansion of the energy gap $\Delta E = E_{3d\pi_g} - E_{2p\pi_u}$ between these states for small R was found long ago [15]

$$\Delta E = \frac{5}{9} - \frac{197}{2835} R^2 + \frac{29190487}{281302875} R^4 + O(R^5), \quad (26)$$

while at large R the corresponding expansion [10] is

$$\Delta E = \frac{1}{2} R^2 e^{-R/2-2} \left(1 + \frac{6}{R} - \frac{40}{R^2} + \dots \right) + O(e^{-R}). \quad (27)$$

Taking numerical data for potential curves of the $2p\pi_u$ and $3d\pi_g$ states (see Table 3 in [2]) we calculate the difference ΔE . This difference is a smooth, slow-changing curve with R , exponentially-vanishing at $R \rightarrow \infty$, see below Fig. 7. Let us make interpolation between small and large distances using the (modified) Padé-type approximation $e^{-R/2-2} \text{Pade}[N + 2/N](R)$ taking for a future convenience $N = 7$,

$$\Delta E = e^{-R/2-2} \frac{5e^2 + a_1 R + a_2 R^2 + a_3 R^3 + a_4 R^4 + a_5 R^5 + a_6 R^6 + R^7}{9 + \alpha_1 R + \alpha_2 R^2 + \alpha_3 R^3 + \alpha_4 R^4 + 2R^5}, \quad (28)$$

with four constraints

$$\begin{aligned} \alpha_1 &= (18 a_1 - 45 e^2)/(10 e^2), \\ \alpha_2 &= (-36 a_1 + 72 a_2 + 3151 e^2/35)/(40 e^2), \\ \alpha_3 &= (152 + 2 a_5 - 12 a_6), \\ \alpha_4 &= (-12 + 2 a_6), \end{aligned} \quad (29)$$

imposed. These constraints guarantee that the appropriate expansions of (28) reproduce correctly the R^0 , R^1 and R^2 terms in (26) and the three terms in (27). After making a fit of the numerical data with (28), the six free parameters are fixed

$$\begin{aligned} a_1 &= 17464. , \quad a_4 = 422.66 , \\ a_2 &= 6995.2 , \quad a_5 = 23.714 , \\ a_3 &= 11.559 , \quad a_6 = -5.7896 , \end{aligned} \quad (30)$$

where all five figures shown are significant. This fit gives, in general, 4-5 figures at the whole range $R \in [0, 40]$ a.u., see Table IV, and up to 8 d.d. for large $R \in [20, 40]$ a.u. (see for illustration Table IV and Fig. 7, blue curve).

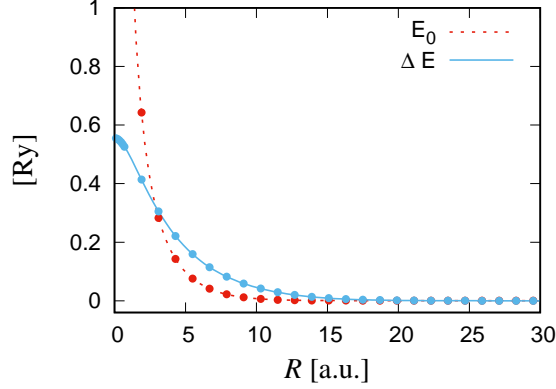


FIG. 7: E_0 and ΔE for the excited states $2p\pi_u$ and $3d\pi_g$. Calculated values indicated by bullets and curves are the fits (37) (dashed line) and (28) (solid line).

1. The dissociation energies

The behavior of the potential curve $E_{2p\pi_u}$ at the two asymptotic limits of small and large distances is well known. For $R \rightarrow 0$ the dissociation energy is given by [15]

$$\tilde{E}_{2p\pi_u}^{(0)} = \frac{2}{R} - \frac{3}{4} + \frac{1}{15}R^2 - \frac{2447}{23625}R^4 + \dots, \quad (31)$$

while for $R \rightarrow \infty$ the expansion reads [8–10]

$$\begin{aligned} \tilde{E}_{2p\pi_u}^{(\infty)} &= \frac{12}{R^3} - \frac{156}{R^4} + \frac{4800}{R^6} + \dots \\ &- \frac{1}{4}R^2 e^{-R/2-2} \left[1 + \frac{6}{R} - \frac{40}{R^2} - \frac{940}{3R^3} - \frac{363}{R^4} + \dots \right] + O(e^{-R}). \end{aligned} \quad (32)$$

Considering now the negative parity state $3d\pi_g$, its expansion for small and large R -distance are also well known,

$$\tilde{E}_{3d\pi_g}^{(0)} = \frac{2}{R} - \frac{7}{36} - \frac{8}{2835}R^2 + \frac{54058}{281302875}R^4 + \dots, \quad (33)$$

at $R \rightarrow 0$, where the term $O(R)$ is absent. The behavior for $R \rightarrow \infty$ is the same as one given by Eq. (32) with sign changed from minus to plus in front of the exponentially-small term $\sim e^{-R/2}$.

Let us consider the half-sum of potential curves for $2p\pi_u$ and $3d\pi_g$ states,

$$E_0 \equiv \frac{\tilde{E}_{2p\pi_u} + \tilde{E}_{3d\pi_g}}{2}. \quad (34)$$

TABLE IV: E_0 and ΔE for the two excited states $E_{2p\pi_u}$ and $E_{3d\pi_g}$ as a function of the internuclear distance R compared to the results of the fits (37) and (28), respectively.

R	$E_0 = \frac{1}{2}(E_{3d\pi_g} + E_{2p\pi_u}) + \frac{1}{4}$		$\Delta E = E_{3d\pi_g} - E_{2p\pi_u}$	
	data	Fit (37)	data	Fit (28)
0.1	19.5280955405	19.528 128	0.5548636236	0.554815
0.5	3.5350863839	3.535 089	0.5395466409	0.539364
1.0	1.5523354867	1.552 324	0.5011027983	0.501303
2.0	0.5945285535	0.594 482	0.4041443865	0.404110
3.0	0.3005373017	0.300 585	0.3135166791	0.313372
4.0	0.1682219136	0.168 226	0.2397424036	0.239864
5.0	0.0985013012	0.098 458	0.1825418518	0.182640
6.0	0.0588028819	0.058 783	0.1389053464	0.138851
7.0	0.0352842264	0.035 295	0.1056662185	0.105586
8.0	0.0210978504	0.021 103	0.0802382260	0.080245
9.0	0.0125143689	0.012 495	0.0606848646	0.060762
10.0	0.0073668353	0.007 341	0.0455988312	0.045662
20.0	0.0005399871	0.000 502	0.0014141722	0.001382
30.0	0.0002547375	0.000 243	0.0000212860	0.000021
40.0	0.0001272650	0.000 125	2.498772×10^{-7}	2.487×10^{-7}

Its corresponding expansions are

$$E_0 = \frac{2}{R} - \frac{17}{36} + \frac{181}{5670}R^2 + O(R^4), \quad (35)$$

at $R \rightarrow 0$, where the linear in R term is absent, and

$$E_0 = \frac{12}{R^3} - \frac{156}{R^4} + \frac{4800}{R^6} + \dots + O(e^{-R}), \quad (36)$$

at $R \rightarrow \infty$, where again the term R^{-5} is absent. The first expansion (35) has a finite radius of convergence, see e.g. [6], while the second one (36) (the half-sum of two multipole expansions) has zero radius of convergence.

Assuming that two-instanton contribution, $\sim e^{-R}$ a large R can be neglected, we construct an analytic approximation for E_0 which mimics the two asymptotic limits (35),

(36). The most convenient way to do it is to use Padé type approximations $E_0(R) = \frac{1}{R}$ Pade[$N/N + 2$](R) with a certain N . Concrete fit was made for $N = 7$, where the Padé approximation is of the form $E_0(R) = \frac{1}{R}$ Pade[7/9](R),

$$E_0 = \frac{2 + R + a_2R^2 + a_3R^3 + a_4R^4 + a_5R^5 + a_6R^6 + 12R^7}{R(1 + \alpha_1R + \alpha_2R^2 + b_3R^3 + b_4R^4 + b_5R^5 + b_6R^6 + \alpha_3R^7 + \alpha_4R^8 + R^9)} , \quad (37)$$

with four constraints imposed,

$$\begin{aligned} \alpha_1 &= 53/72 , \\ \alpha_2 &= (901 + 2592a_2)/5184 , \\ \alpha_3 &= (a_5 + 13a_6 + 2028)/12 , \\ \alpha_4 &= (a_6 + 156)/12 , \end{aligned} \quad (38)$$

in order to guarantee that the three coefficients in front of R^{-1} , R^0 and R^1 of expansion at $R \rightarrow 0$, see (35) and the three coefficients in front of R^{-3} , R^{-4} and R^{-5} at $R \rightarrow \infty$, in the $1/R$ -expansion (36) are exact. Thus, (37) depends on nine free parameters. After making the fit with (37), we arrive to concrete values of these nine free parameters:

$$\begin{aligned} a_2 &= 677043. , \quad b_3 = 107330. , \\ a_3 &= 54874.3 , \quad b_4 = 21319.7 , \\ a_4 &= -8925.37 , \quad b_5 = -839.229 , \\ a_5 &= 2332.69 , \quad b_6 = 703.849 , \\ a_6 &= -296.134 . \end{aligned} \quad (39)$$

It provides not less than 4-6 figures in E_0 for whole studied domain $R \in [1, 40]$ a.u. (see Table IV and Fig. 7).

The potential curve for the $2p\pi_u$ state can be constructed from (37) and (28) by taking

$$E_{2p\pi_u} = E_0 - \frac{1}{2}\Delta E . \quad (40)$$

This expression reproduces 4-5-6 figures in energy for the whole domain $R \in [0, 40]$ a.u., when comparing with the exact values (see Table 3 in [2]). For illustration see Fig. 8. The fit predicts the minimum of the potential curve as $E_{min} = -0.269\,022$ Ry (cf. $E_{min}^{exact} = -0.269\,027\,6$ Ry (rounded)) while its location is $R_{eq} = 7.957$ a.u. (c.f. $R_{eq}^{exact} = 7.931$ a.u.). Due to the dominant long range interaction is repulsion $\sim 12/R^3$ (see (32)) the potential curve should display a maximum. Again, it is noticeable that the fit predicts the maximum

of the potential curve as $E_{max} = -0.249\,734$ Ry (c.f. $E_{max}^{exact} = -0.249\,713$ Ry (rounded)) which is localized at $R_{max} = 26.138$ a.u. (c.f. $R_{max}^{exact} = 25.809$ a.u. (rounded)).

The asymptotic expansions of Eq. (40) are given by

$$\tilde{E}_0 = \frac{2}{R} - \frac{3}{4} + 71.8 R^2 + \dots, \quad (41)$$

$$\tilde{E}_\infty = \frac{12}{R^3} - \frac{156}{R^4} - \frac{10729.2}{R^6} + \dots - \frac{1}{4} R^2 e^{-R/2-2} \left[1 + \frac{6}{R} - \frac{40}{R^2} - \frac{645.2}{R^3} + \dots \right], \quad (42)$$

which are in complete agreement with the first three terms at $R \rightarrow 0$ and $R \rightarrow \infty$ (in the $1/R$ expansion of the pre-factor to $e^{-R/2}$, cf. (31) and (32)).

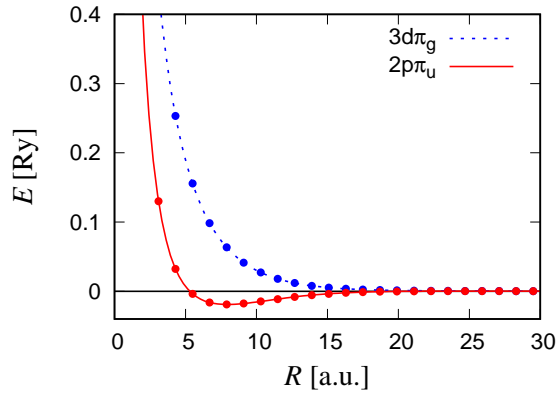


FIG. 8: Potential curve for the excited states $2p\pi_u$ (solid line) and $3d\pi_g$ (dotted line): points are the calculated values and the curves are the fits (40) and (43), respectively.

Similarly, the potential curve for the excited state $3d\pi_g$ is restored from (37) and (28) by taking

$$E_{3d\pi_g} = E_0 + \frac{1}{2} \Delta E. \quad (43)$$

This expression also reproduces 4-6 figures when comparing with the exact energy, see Table 3 in [2] and for illustration Fig. 8. The asymptotic expansions of Eq. (43) are given by

$$\tilde{E}_0 = \frac{2}{R} - \frac{7}{36} + 71.7 R^2 + \dots, \quad (44)$$

$$\tilde{E}_\infty = \frac{12}{R^3} - \frac{156}{R^4} - \frac{10729.2}{R^6} + \dots + \frac{1}{4} R^2 e^{-R/2-2} \left[1 + \frac{6}{R} - \frac{40}{R^2} - \frac{645.2}{R^3} + \dots \right], \quad (45)$$

which are in complete agreement with the first three terms at $R \rightarrow 0$ (cf. (33)), and in both three terms in $1/R$ expansion and three terms in $1/R$ expansion of the pre-factor to $e^{-R/2}$ for $R \rightarrow \infty$ (cf. (32)). This potential curve displays no minimum, thus, the state $3d\pi_g$ is pure repulsive.

2. *Vibrational states associated with the potential curve $2p\pi_u$*

Taking the function (40) as the potential $V(R)$ for the $2p\pi_u$ -state, we calculate the rovibrational bound states by solving (25) at different L . In order to solve this one-dimensional differential equation the Lagrange-mesh method is used [11] as for $1s\sigma_g$. Table V presents the obtained rovibrational states for $L = 0, 4$, where the reduced mass of the two protons was taken equal to $\mu = 918.048$. This potential well keeps 12 vibrational states at $L = 0$ and 284 rovibrational states in total, see Figure 9. Beckel et al. [16] reported vibrational states for $L = 1, 4, 8, 12, 16$ where the first correction to the Born-Oppenheimer approximation was included. At $L = 4$ our results differ from [16] systematically at 5th figure which likely the order of the contribution of the first correction to the Born-Oppenheimer approximation. Maximum angular momentum L , which still keeps vibrational bound state, is equal to $L_{max} = 36$.

We are not aware about any calculations beyond of the Bohr-Oppenheimer approximation for the state $2p\pi_u$. It seems likely that some rovibrational states can exist.

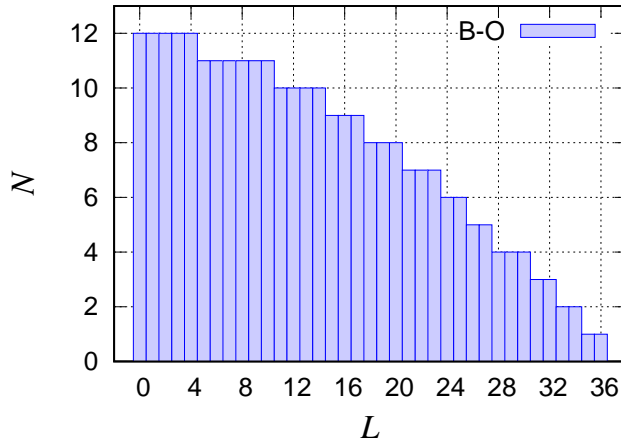


FIG. 9: Number of vibrational states supported by the excited state $2p\pi_u$ as a function of the angular momentum L , here $L_{max} = 36$. In total, there are 284 rovibrational states.

TABLE V: Rovibrational energies $E_{\nu L}$ of the excited state $2p\pi_u$ at $L = 0, 4$. For $L = 4$ the second line are the results from [16]. This potential curve has a maximum E_{max} at

$R = 25.809$ a.u. (rounded)

ν	$E_{\nu 0}[\text{Ry}]$	$E_{\nu 4}[\text{Ry}]$
0	-0.267 83	-0.267 50
		-0.267 507 4
1	-0.265 54	-0.265 22
		-0.265 214 9
2	-0.263 35	-0.263 04
		-0.263 043 8
3	-0.261 28	-0.260 98
		-0.260 997 7
4	-0.259 33	-0.259 05
		-0.259 081 0
5	-0.257 52	-0.257 25
		-0.257 299 3
6	-0.255 84	-0.255 60
		-0.255 659 9
7	-0.254 33	-0.254 10
		-0.254 171 9
8	-0.252 98	-0.252 78
		-0.252 847 5
9	-0.251 82	-0.251 64
		-0.251 702 4
10	-0.250 87	-0.250 71
		-0.250 759 0
11	-0.250 16	-0.250 04
		-0.250 052 4
E_{diss}		-0.25
E_{min}		-0.269 027 6
E_{max}		-0.249 712 8

III. THE GROUND STATE $X^2\Sigma^+$ OF THE HeH MOLECULE

The analysis implemented above for the homonuclear molecule H_2^+ can also be extended to the case of heteronuclear molecules. As an example, let us consider the simplest neutral diatomic molecule made up of a Helium atom plus a Hydrogen atom, the (HeH) molecule. The potential curve for the ground state as a function of the internuclear distance $E(R)$ is repulsive with a shallow van der Waals minimum at $R = 6.66$ a.u. [17], [4]. The united atom limit $R \rightarrow 0$ evidently corresponds to the Li atom while at large internuclear distances the HeH molecule dissociates like $HeH \rightarrow He + H$. The dissociation energy is given by

$$\tilde{E} = E(R) - (E_{He} + E_H), \quad (46)$$

where $E_{He} = -8.71017$ a.u. and $E_H = -0.99946$ a.u. [18].

The dissociation energy \tilde{E} for small internuclear distances $R \rightarrow 0$ can be expanded as [15]

$$\tilde{E} = \frac{4}{R} - \varepsilon_0 + O(R^2) + \dots, \quad (47)$$

where the first term is the repulsive interaction $2Z_1Z_2/R$ while the term ε_0 corresponds to the absolute value of the united atom energy minus sum of the energies of H and He, $\varepsilon_0 = |E_{Li} - (E_{He} + E_H)| = 8.14972$ Ry. As was pointed long ago by Buckingham [19] the linear term $\sim R$ should be absent. At large internuclear distances $R \rightarrow \infty$ the dissociation energy is expanded as [20]

$$\tilde{E} = -\frac{C_6}{R^6} - \frac{C_8}{R^8} - \frac{C_{10}}{R^{10}} + \dots, \quad (48)$$

where the (rounded) coefficients C_i are $C_6 = 5.64268$, $C_8 = 83.6728$ and $C_{10} = 1743.080$ in a.u. For our purposes it has to be paid attention that the term $\sim 1/R^7$ is absent.

Now, in order to construct an analytic approximation of the potential curve which mimics the two asymptotic limits (47) and (48) a Padé type (meromorphic) approximation of the form $E(R) = \frac{1}{R}\text{Pade}[N/N+5](R)$ is used. Taking $N = 4$, which seems appropriate for our purposes, the explicit expression for $E(R) = \frac{1}{R}\text{Pade}[4/9](R)$ is

$$E = \frac{(4 + a_1R + a_2R^2 + a_3R^3 - C_6R^4)}{R(1 + \alpha_1R + \alpha_2R^2 + b_3R^3 + b_4R^4 + b_5R^5 + b_6R^6 - \alpha_3R^7 - \alpha_4R^8 + R^9)}, \quad (49)$$

with four constraints

$$\begin{aligned}
\alpha_1 &= (a_1 + \varepsilon_0)/4, \\
\alpha_2 &= (-a_1\varepsilon_0 + \varepsilon_0^2 + 4a_2)/16, \\
\alpha_3 &= (a_2 + C_8)/C_6, \\
\alpha_4 &= a_3/C_6.
\end{aligned}
\tag{50}$$

which guarantee that the coefficients in front of R^{-1} , R^0 and R^1 at small internuclear distances in (47) and the coefficients in front of R^{-6} , R^{-7} and R^{-8} for large internuclear distances in (48) are reproduced exactly. After making a fit with the analytic expression (49), using the numerical energy values reported by Murrell *et al.* [4], the values of the remaining seven free parameters are

$$\begin{aligned}
a_1 &= 2072.1784, & b_3 &= 2075.4703, \\
a_2 &= -604.31543, & b_4 &= -2101.4132, \\
a_3 &= 76.347450, & b_5 &= 1152.5705, \\
&& b_6 &= -380.63678.
\end{aligned}
\tag{51}$$

Expression (49) provides 6-9 figures in the total energy as can be seen in Table VI. Taking the derivative of (49) the minimum of the potential curve is predicted as $E_{min}^{(fit)} = -6.80628$ Ry (c.f. $E_{min} = 6.80629$ Ry from [17]) at $R_{min}^{(fit)} = 6.707$ a.u. (c.f. $R_{min} = 6.660$ a.u. from [17]). Figure 10 displays the analytic potential (49) as well as the theoretical energy values used to make the fit [4] (blue circles). Comparison with results by Meyer *et al.* [17] (red triangles) are also depicted. The small plot in Figure 10 amplifies the details of the curve around the shallow minimum.

The asymptotic expansions of Eq. (49) are given by

$$E_0 = \frac{4}{R} - 8.14972 - 821.0904 R^2 + \dots \tag{52}$$

$$E_\infty = -\frac{5.64268}{R^6} - \frac{83.6728}{R^8} - \frac{1207.756}{R^9} + \dots, \tag{53}$$

which reproduce the first three term of R^{-1} , R^0 and R for $R \rightarrow 0$ (see (47)) and the first three terms R^{-6} , R^{-7} and R^{-8} for $R \rightarrow \infty$ (see (48)).

The traditional molecular system (HeH) has been studied numerically for a long time, see Murrell *et al.* [4] and references therein. We do not think that numerical studies are completed and we have fully reliable results. There are always a certain controversies between

TABLE VI: Total energy E_0 for the ground state of the HeH molecule as a function of the internuclear distance R in a.u. Second column corresponds to the results presented in [4] and third column are the results of the fit (49).

R	$E_0 \times 10^{-6}[\text{Ry}]$	
	data	Fit
1.890	147183.334	147183.306
2.835	33875.651	33875.635
4.252	2633.407	2633.024
6.047	-16.548 610	-16.299
6.236	-31.985 473	-31.646
6.425	-39.813 257	-39.475
6.614	-42.765 763	-42.492
6.803	-42.674 636	-42.528
6.992	-40.806 539	-40.800
7.181	-37.954 273	-38.107
10.393	-5.075 757	-5.474
12.283	-1.795 196	-1.934
14.173	-0.738 126	-0.790
16.063	-0.346 281	-0.362
18.897	-0.127 577	-0.133
22.677	-0.041 918	-0.0434
26.456	-0.016 403	-0.0170
30.236	-0.007 290	-0.0076
37.795	-0.001 823	-0.00196

different calculations. E.g. for total energy at $R = 6.0$ a.u. data by Meyer *et al.* [17] differ from Murrell *et al.* [4] with the relative difference is $\sim 30\%$. Although for other values of R the relative difference varies in $\lesssim 7 \cdot 10^{-2}$. Making fit to find parameters in (49) we used data by Murrell *et al.* [4] excluding the point $R = 6.0$ a.u.

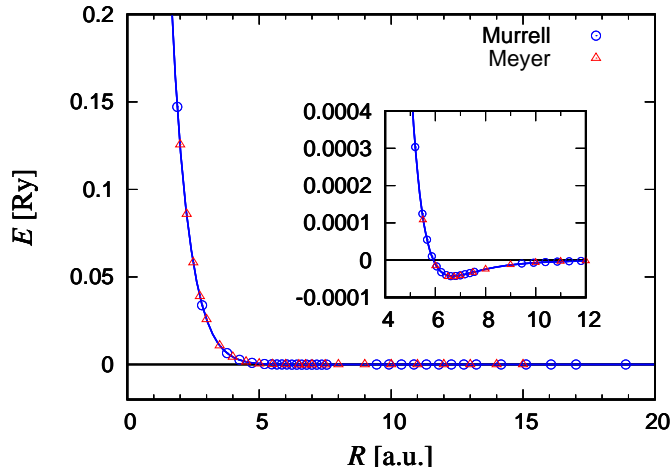


FIG. 10: Dissociation energy of the ground state of the HeH molecule. The solid curve is the fit (49) compared with theoretical calculations by Murrell *et al.* [4] and Meyer *et al.* [17]. The van der Walls minimum (amplification) is located at $R \approx 6.7$ a.u.

Recently, a certain fit of the potential curve was proposed by Warnicke *et al.* [18]. When comparing our fit (49) with the fit V_{TT2} [18], the relative difference goes from $\sim 1\%$ for large R up to $\sim 30\%$ for small $R \sim 1$ a.u.. The main deficiency of the V_{TT2} potential is the wrong description of the asymptotic behavior for $R \rightarrow 0$ and $R \rightarrow \infty$, as one can see by expanding V_{TT2} .

The analytic expression for the potential curve of the ground state $X^2\Sigma^+$ together with (25) allows us to calculate possible rovibrational states supported by the shallow minimum. Using the Lagrange-mesh method to solve (25) we claim that the ground state does not keep any rovibrational state(!) confirming what was already mentioned in numerical studies, see [4].

Conclusions

Using accurate analytic approximations of the potential curves for $1s\sigma_g$ and $2p\sigma_u$, $2p\pi_u$ and $3d\pi_g$ states of H_2^+ for the whole domain in interproton distance R we study vibrational, rotational and rovibrational states. It is shown that the ground state $1s\sigma_g$ can keep 420 rovibrational states within Bohr-Oppenheimer approximation which accuracy is limited to 3-4-5 figures. Going beyond the Bohr-Oppenheimer approximation to the full geometry, where

finite mass effects are taken into account, the number of these states increases surprisingly little, to 423, see [13]. As for vibrational states this number goes from $\nu = 19$ to $\nu = 20$. At the same time as for the state $2p\sigma_u$ the total number of rovibrational states (all with $\nu = 0$) is equal to 3 within or beyond Bohr-Oppenheimer approximation. For the state $2p\pi_u$ within the Bohr-Oppenheimer approximation the number of vibrational states is equal to 12 while the total number of the rovibrational bound states is equal to 284. The potential curve for the state $3d\pi_g$ displays no minimum, thus, the state $3d\pi_g$ is pure repulsive.

The same procedure was applied to the ground state $X^2\Sigma^+$ of the heteronuclear system HeH. The approximation of the potential curve gives better description of the electronic energy than any previous approximation. The shallow minimum at $R \approx 6.6$, presented by the potential curve does not keep rovibrational states. Can developed procedure of interpolation work for other heteronuclear systems as well as homonuclear systems will be studied elsewhere. So far, one can only be surprised that such a simple, straightforward interpolation provides so accurate description of potential curves for H_2^+ and (HeH).

Acknowledgements.

H.O.P. is grateful to Instituto de Ciencias Nucleares, UNAM (Mexico) for a kind hospitality extended to him where a certain stages of the present work were carried out. The research by A.V.T. is supported in part by PAPIIT grant **IN108815** (Mexico).

-
- [1] L.D. Landau and E.M. Lifshitz,
Quantum Mechanics, Non-relativistic Theory (Course of Theoretical Physics vol 3),
3rd edn (Oxford:Pergamon Press), 1977
- [2] H. Olivares-Pilón and A.V. Turbiner,
The H_2^+ molecular ion: Low-lying states,
Ann. Phys. **373** (2011) 5821-608
- [3] A.V. Turbiner and H. Olivares-Pilón,
The H_2^+ molecular ion: a solution,
J. Phys. B **44** 101002 (7 pp) (2011)

- [4] J. N. Murrell, T. G. Wright, and S. D. Bosanac,
*A search for bound levels of the van der waals molecules: $H_2(\alpha^3\Sigma_u^+)$, $HeH(X^2\Sigma^+)$, $LiH(\alpha^3\Sigma^+)$
and $LiHe(X^2\Sigma^+)$,*
J. Mol. Struct.: THEOCHEM **591**, 1-9 (2002)
- [5] W. Byers Brown and E. Steiner,
On the Electronic Energy of a One-Electron Diatomic Molecule near the United Atom,
J. Chem. Physics **44**, 3934-3940 (1966)
- [6] M. Klaus,
On H_2^+ for small internuclear separation,
J. Phys. A: Math, Gen. **16**, 2709-2720 (1983)
- [7] W. Byers Brown, *Interatomic Forces at Very Short Range,*
Discussions Faraday Soc. **40** 140-149, (1965)
- [8] A.A. Ovchinkikov, and A.D. Sukhanov,
Dokl.Akad.Nauk, SSSR, **157**, 1092-1095 (1964),
Soc.Phys.-Dokl. **9**, 685-687 (1965)(English translation)
- [9] R.J. Damburg and R.Kh. Propin,
On asymptotic expansions of electronic terms of the molecular ion H_2^+ ,
J. Phys. B. (Proc Phys. Soc.) **1** , 4, 681-691 (1968)
- [10] J. Cizek et al.,
1/R expansion for H_2^+ : Calculation of exponentially small terms and asymptotics,
Phys. Rev. A **33**, 12 - 54 (1986)
- [11] D. Baye,
The Lagrange-mesh method,
Phys. Repts. **565**, 1-107 (2015)
- [12] C.L. Beckel, B.D. Hansen III and J.M. Peek,
Theoretical study of H_2^+ ground electronic state spectroscopic properties,
J. Chem. Phys **53**, 3681-3690 (1970)
- [13] R. Moss,
*Calculations for the vibration-rotation levels of H_2^+ in its ground and first excited electronic
states,*
Mol. Phys. **80**, 1541-1554 (1993)

- [14] J.M. Peek,
Discrete Vibrational States Due Only to Long Range Forces: $^2\Sigma_u^+$ ($2p\sigma_u$) State of H_2^+ ,
J. Chem. Phys **50**, 4595-4696 (1969)
- [15] W.A. Bingel,
United atom treatment of the behavior of potential energy curves of diatomic molecules for small R ,
J. Chem. Phys **30**, 1250-1253 (1958)
- [16] C.L. Beckel, M. Shafi and J.M. Peek,
Theoretical study of H_2^+ spectroscopic properties. II. The $2p\pi_u$ electronic state,
J. Chem. Phys **59**, 5288-5297 (1973)
- [17] W. Meyer and L. Frommhold
Long-range interactions in H-He: ab initio potential, hyperfine pressure shift and collision-induced absorption in the infrared,
Theor. Chim. Acta **88**, 201-216 (1994)
- [18] S. Warnicke, K.T. Tang, and J.P. Toennies,
Communication: Simple full range analytic potential for H_2 , H-He, He_2 ,
J. Chem. Phys **142** 131102 (2015)
- [19] R.A. Buckingham,
Trans. Faraday Soc. **54**, 453 (1958)
- [20] Z.C. Yan, J.F. Babb, and A. Dalgarno,
Variational calculations of dispersion coefficients for interactions among H, He, and Li atoms,
Phys. Rev. A **54**, 2824-2836 (1996)
- [21] Due to controversy in literature we use in [2] a slightly incorrect coefficient (in $\sim 1\%$) in front of R^2 term: $\frac{27}{5}$. It did not really lead to a change of conclusions in [2]
- [22] Note for completeness that beyond the Born-Oppenheimer approximation Moss [14] reported 14 quasi-bound rovibrational states for $L > 35$ and 44 quasi-bound rovibrational states for $L \leq 35$. The questions related to the existence of quasi-bound states are beyond the scope of the present paper